

Affordance-Guided Reinforcement Learning via Visual Prompting

Olivia Y. Lee¹, Annie Xie¹, Kuan Fang², Karl Pertsch^{1,3}, Chelsea Finn¹

Abstract—Robots equipped with reinforcement learning (RL) have the potential to learn a wide range of skills solely from a reward signal. However, obtaining a robust and dense reward signal for general manipulation tasks remains a challenge. Existing learning-based approaches require significant data, such as human demonstrations of success and failure, to learn task-specific reward functions. Recently, there is also a growing adoption of large multi-modal foundation models for robotics that can perform visual reasoning in physical contexts and generate coarse robot motions for manipulation tasks. Motivated by this range of capability, in this work, we present **Keypoint-based Affordance Guidance for Improvements (KAGI)**, a method leveraging rewards shaped by vision-language models (VLMs) for autonomous RL. State-of-the-art VLMs have demonstrated impressive reasoning about affordances through keypoints in zero-shot, and we use these to define dense rewards that guide autonomous robotic learning. On real-world manipulation tasks specified by natural language descriptions, KAGI improves the sample efficiency of autonomous RL and enables successful task completion in 20K online fine-tuning steps. Additionally, we demonstrate the robustness of KAGI to reductions in the number of in-domain demonstrations used for pre-training, reaching similar performance in 35K online fine-tuning steps.[†]

I. INTRODUCTION

Recent advances in large language models (LLMs) and vision-language models (VLMs) trained on Internet-scale data show promising results in using commonsense understanding to plan and reason [1]–[5]. They can break down complex instructions provided in natural language into actionable task plans [3], [6]–[10], perform visual reasoning in a variety of contexts [11]–[13], and even generate coarse robot motions for simple manipulation tasks [7], [9], [13]–[16]. However, state-of-the-art models still struggle with understanding 3D physical dynamics and interactions, which is essential to robotic control. Several prior works have utilized large pre-trained models for robotic control, either through few-shot prompting or fine-tuning of large models to generate actions directly [7], plans [3], [9], [10], or code [17], [18]. However, fine-tuning typically requires extensive human supervision, such as teleoperated demonstrations, feedback on whether the task was successfully completed, or a predefined set of skills and their controllers.

An alternative paradigm for fine-tuning robotic policies is autonomous reinforcement learning (RL), which only requires a reward signal to refine the robot’s behavior and can therefore require less supervision in comparison. A significant amount of recent work has also focused on improving the sample efficiency of these algorithms by pre-training on

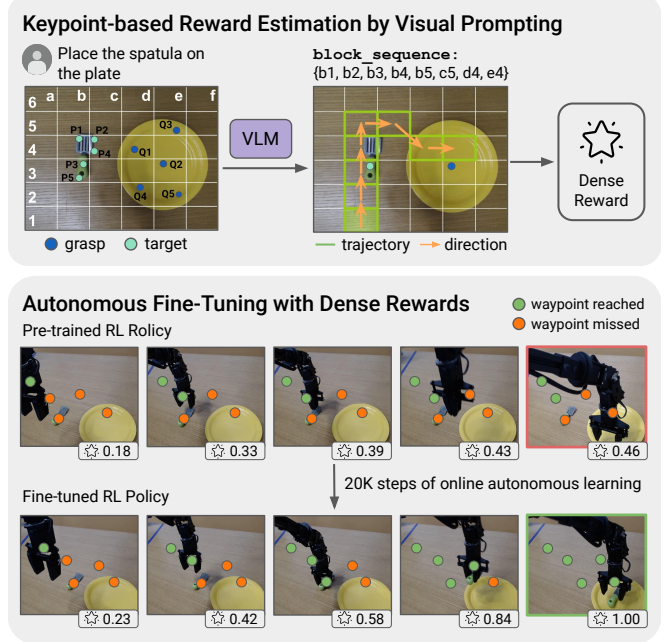


Fig. 1: Keypoint-based Affordance Guidance for Improvements (KAGI) computes dense rewards defined using affordance-based keypoints and waypoints trajectories inferred by a VLM. Our dense reward formulation helps to shape learned behaviors, facilitating efficient online fine-tuning across diverse real-world tasks.

large offline datasets [19]–[24]. Despite these advances, obtaining a reward signal is still a non-trivial problem, requiring either careful engineering or large amounts of data to learn a robust reward function [25]–[29]. The potential of using pre-trained VLMs to define rewards is hence attractive, but thus far, they have primarily been used for generating sparse rewards [24], [30], [31], which often leads to less efficient learning. VLMs hold much richer and denser knowledge that we can elicit, such as reasoning about the affordances of various objects and environments. In this work, we leverage this understanding to shape rewards for robotic RL.

We present **Keypoint-based Affordance Guidance for Improvements (KAGI)**, a method for open-vocabulary visual prompting to extract rewards from VLMs for autonomous RL. We leverage insights on effective visual prompting techniques [11], [32] to generate affordance keypoints and waypoint trajectories, from which we derive dense shaping rewards for online fine-tuning. As shown in Fig. 1, we integrate our pipeline of extracting affordance keypoint representations from VLMs and computing waypoint-based dense rewards into RoboFuME [24], an autonomous RL system that uses sparse rewards from a fine-tuned VLM.

¹Stanford University, ²Cornell University, ³University of California, Berkeley. Correspondence to: oliviayl@stanford.edu

[†]Project page: sites.google.com/view/affordance-guided-rl

We demonstrate improved success rates on complex object manipulation tasks that the system using only sparse rewards struggles to generalize to, with reduced reliance on in-domain expert demonstrations.

II. RELATED WORK

A. Foundation Models for Robotics

Planning and high-level reasoning. The rapid development of foundation models in recent years has drawn significant attention [33]. This surge of interest has arisen because foundation models demonstrate that models trained on broad, Internet-scale data are highly adaptable to a wide range of downstream tasks. Robotics is a specific downstream task of foundation models that has garnered a lot of interest in the academic community. Foundation models have enabled high-level planning and reasoning for embodied agents [3], [9], [10], [34]–[37], generated sub-goals [38]–[40], and generated coarse motions for manipulation [9], [13]–[16], [41]. These impressive results across a wide range of domains demonstrate great potential in harnessing the rich knowledge and reasoning capabilities of foundation models to enable embodied agents to complete long-horizon tasks.

Despite the rapid development of LLMs for robotic control, recent works have investigated using multi-modal models to jointly provide visual and language prompts to robotic agents [6], [13], [16], [42]. These approaches recognize that converting visual observations into language descriptions and planning solely with language loses rich information associated with the visual modality for scene understanding, a major limitation of using LLMs for spatial planning, reasoning, and task completion. Though LLMs can provide general priors for planning and reasoning, they must be properly grounded to generate accurate responses about real world environments [43]–[47]. Our work explores harnessing state-of-the-art VLMs to facilitate reasoning in both language and image domains. We leverage the image domain by computing rewards in image space, using this to bridge high-level LLM plans with low-level actions for embodied tasks.

Spatial reasoning with VLMs. The clear advantage of language is the natural interface for providing task instructions and specifying goals. That said, robotics relies heavily on accurately perceiving and interacting with the environment. Modern VLMs, such as GPT-4V [48] and Gemini [49], demonstrate promising capabilities in combining reasoning with environment perception via visual inputs. Recent works have leveraged this capability to perform keypoint-based reasoning [32], [50] and mark-based visual prompting for zero-shot manipulation [11], [13], [32]. Such approaches facilitate the process of translating high-level plans into low-level robot actions. Beyond zero-shot manipulation, our work explores deriving rewards from VLMs to improve online RL.

Modern VLMs can derive rewards in image space by determining success or failure based on image observations. These reward signals can be used for learning state-action mappings via RL, enabling robots to learn through trial-and-error, without training skill policies via imitation learning which are costly and difficult to scale. VLMs can also

guide learning by generating shaping rewards in the form of waypoint trajectories. A key contribution of our work is using VLMs to both determine task completion and specify intermediate waypoints as goals. A major engineering challenge is tuning the inputs to VLMs, which are highly expressive but also opaque, to derive useful reward signals for learning. Both language and image prompts must be tuned to generate accurate and meaningful outputs, as modern VLMs still struggle somewhat with spatial reasoning using raw inputs. Our work explores using the outputs of preliminary VLMs (e.g., bounding boxes [51] and segmentations [52]) to augment raw image observations as guidance for semantic reasoning in more advanced VLMs, thereby leveraging pre-trained representations in VLMs as reward predictors.

B. Autonomous Reinforcement Learning

Online RL is the paradigm by which an agent gathers data through interaction with the environment, then stores this experience in a replay buffer to update its policy. This contrasts with offline RL, where an agent updates its policy using previously collected data without itself interacting with the environment. A longstanding goal is autonomous RL, an agent that autonomously gathers real-world experience, which holds great promise for scalable robot learning. Agents not only learn through their own experience, but also do not require manual environment resets between trials [53].

Algorithms for autonomous RL are difficult to implement in the real world, with the primary challenges being sample complexity, providing well-shaped rewards, and continual reset-free training. Several works have developed reset-free systems that reduce or eliminate human interventions [24], [54]–[56], but reward shaping is an open problem. Manually specified rewards are difficult to engineer and easy to exploit. While hand-designing reward functions is challenging, there is great potential to learn rewards from previously collected data or large pre-trained models. The large bank of offline image and video datasets, plus the high inference speed and accessibility of large pre-trained models, could provide more precise and informative shaping rewards.

RoboFuME [24] is a recent work that fine-tunes MiniGPT-4 [57] to generate sparse task completion rewards for autonomous RL. However, autonomous RL suffers when reward signals are too sparse, and fine-tuning MiniGPT-4 requires a substantial number of in-domain demonstrations per task, which is costly but also makes the system more brittle and less robust to generalization. We draw upon recent work that explores extracting rewards from LLMs [58], [59] and VLMs to guide zero-shot robotic manipulation [30]–[32] and online adaptation [24], [60]. In particular, our work leverages affordance representations extracted from VLMs to tackle the dense reward shaping problem.

III. KEYPOINT-BASED AFFORDANCE GUIDANCE FOR IMPROVEMENTS (KAGI)

A. Problem Statement

We propose Keypoint-based Affordance Guidance for Improvements (KAGI) to facilitate autonomous fine-tuning on

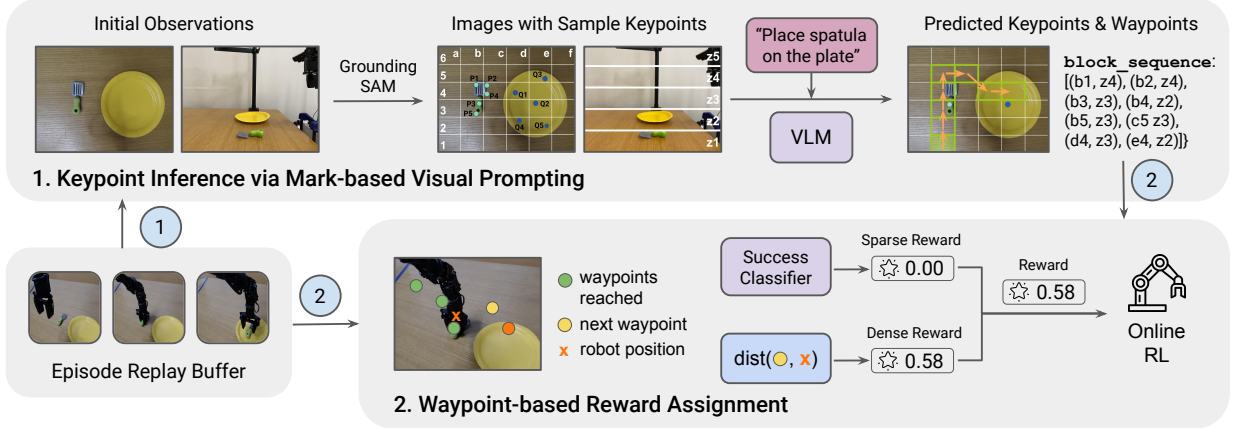


Fig. 2: **KAGI** consists of two components. The first, represented by arrow labeled 1 above, leverages a VLM to select from a set of affordance keypoints, then generate a waypoint sequence. The second, represented by arrows labeled 2 above, involves per timestep reward computation for each frame in the episode replay buffer, computing dense reward with respect to the waypoint sequence and a sparse reward derived from a success classifier. The dense reward is used for online RL if the sparse reward is 0, else the sparse reward is used.

unseen tasks as shown in Fig. 2. We consider problems that can be formulated as a partially observable Markov Decision Process (POMDP) tuple $(\mathcal{S}, \mathcal{A}, \mathcal{O}, \gamma, f, p, r, d_0)$ where \mathcal{S} is the state space, \mathcal{A} is the action space, \mathcal{O} is the observation space, $\gamma \in (0, 1)$ is the discount factor, $r(s, a)$ is the reward function and $d_0(s)$ is the initial state distribution. The dynamics are governed by a transition function $p(s'|s, a)$. The observations are generated by an observation function $f(o|s)$. The goal of RL is to maximize the expected sum of discounted rewards $\mathbb{E}_\pi[\sum_{t=1}^{\infty} \gamma^t r(s_t, a_t)]$. In this work, we use RGB image-based observations. The reward function is typically hand-engineered or learned, for instance via examples of task success and failure [24]–[29]. We assume the existence of a sparse task completion reward (i.e., $r(s, a) \in \{0, 1\}$), acquired with systems like RoboFuME [24].

Our system consists of an offline pre-training phase and an online fine-tuning phase, where the latter phase requires a reward function to label successes and failures. A sparse reward is typically easier to specify but, with it, RL algorithms require more samples to learn a successful policy, because the agent must encounter success through its own exploration. In comparison, a dense reward provides continuous feedback that guides the agent towards success. KAGI aims to provide the latter type of feedback by augmenting sparse task completion rewards with dense shaping rewards. Specifically, dense rewards are calculated with respect to intermediate waypoints marking trajectory points towards the goal. We find that such guidance can facilitate more efficient and generalizable online learning than sparse rewards alone.

B. Keypoint-Based Reward Estimation via Visual Prompting

We employ a vision language model (VLM) to estimate dense rewards to facilitate fine-tuning of a pre-trained policy. First, we prompt the VLM to select appropriate grasp and target keypoints for the task, inspired by recent visual prompting techniques [32]. Then, the estimated rewards are used to generate a coarse trajectory of how the robot should complete the task. We then assign rewards to each timestep of an RL episode based on how well it follows this trajectory.

We take the first observation in the episode o_0 , consisting of a top-down image o_0^d and a side view image o_0^s . Our goal is to create a candidate set of grasp and target keypoints that GPT-4V can select from. We preprocess these images by (1) passing o_0^d through GroundingSAM to get segmentations of relevant objects and sample five points from their masks, and (2) overlaying a 6×6 grid and the sampled keypoints on top of o_0^d to get \tilde{o}^d . For the side-view image, we augment o_0^s with evenly-spaced labeled horizontal lines to get \tilde{o}^s , providing depth information not available in the top-down view. See Figures 3a and 3b as examples. We use this density of grid lines as [32] and preliminary tests found that this was most suitable for GPT-4V to reason with. We pass \tilde{o}^d and \tilde{o}^s with a language instruction and metaprompt to GPT-4V, which generates `block_sequence`. This sequence is a list of tuples (x, y, z) , where (x, y) is a grid point chosen from \tilde{o}^d representing a position in the xy-plane from top-down and z is chosen from \tilde{o}^s representing height in the z-axis from the side view. Dense rewards are calculated with respect to `block_sequence` in the next step.

For each frame in the episode, we compute the robot position in image space. We use two fitted RANSAC regressors, one for each camera view, to compute the robot position $(x_{\text{rob}}^t, y_{\text{rob}}^t, z_{\text{rob}}^t)$, where $(x_{\text{rob}}^t, y_{\text{rob}}^t)$ is from the top-down and z_{rob}^t is from the side view. Optionally, we can use pixel trackers [61] to track a specific point on the object $(x_{\text{obj}}^t, y_{\text{obj}}^t, z_{\text{obj}}^t)$ to additionally define rewards based on object poses. Using these coordinates, we compute the nearest block to the robot position in `block_sequence`, B_{rob}^i (see Figure 3c for an example). We compute a reward r_{rob}^t is based on the L2 distance from the robot position to the *block after the closest block in block_sequence*, B_{rob}^{i+1} . We use the next block to encourage progression towards the goal and avoid stagnating at the current position. We transform the distance such that reward is between 0 and 1: $r_t = 0.5 \cdot (1 - \tanh(\text{dist}))$. The reward is 1 when the sparse reward is 1, otherwise it is our dense reward. This reward is then optimized with an online RL algorithm.

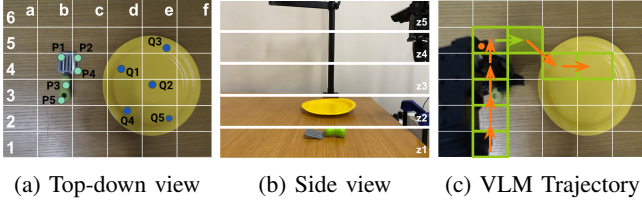


Fig. 3: Example of annotated images to VLM (3a, 3b) and VLM-generated trajectory (3c). In 3a, teal points labeled P1-5 denote grasp keypoints, blue points labeled Q1-5 denote target keypoints for the VLM to select from. In 3c, orange point is robot position, green tiles denote the generated trajectory, and arrows denote motion direction. KAGI’s dense reward formulation encourages the robot to move to the next block, following the green arrow.

We query GPT-4V once at the start of each experiment to generate the affordance keypoints and intermediate waypoints for the forward and backward tasks, which we use for all forward and backward episodes. This is primarily because querying GPT-4V after every episode incurs a prohibitively high cost, but we found that the trajectory is coarse enough to be robust to small randomizations in environment resets.

C. System Summary

To optimize this reward, we build on RoboFuME [24], an autonomous RL pipeline that learns from image observations. RoboFuME requires a set of forward and backward task demonstrations, and pre-trains a policy on this data and the Bridge dataset [62], [63]. For the reward model, it fine-tunes MiniGPT-4 [57] as a success classifier using the in-domain demonstrations and a few additional failure examples. We augment these sparse rewards with our waypoint-based dense rewards to combine the benefits of both modes of feedback.

From the VLM-generated waypoint trajectory, we use the centroid of each grid tile and height from the side-view to create a 3D coordinate trajectory. We calculate the L2 distance between the current robot position and target waypoint in image space, and pass each distance through a modified tanh function, so $r_{\text{dense}} = 0.5(1 - \tanh(\lambda(d_t - \varphi)))$, where d_t is the L2 distance between the robot position and target waypoint at timestep t . The scaling factor λ and offset φ are hyperparameters; $\lambda = 0.1$, $\varphi = 15$ for the simulation experiments in Section IV-B, and $\lambda = 0.02$, $\varphi = 100$ for the real-robot experiments in Section IV-C. This ensures the dense reward stays between 0 and 1, with values closer to 1 when the robot trajectory is closer to the VLM-generated waypoint trajectory. What distinguishes trajectories that stay close to the VLM-generated trajectories and truly successful trajectories is the sparse reward. We set the final reward for each timestep $r = r_{\text{sparse}}$ if $r_{\text{sparse}} = 1$ else $r = r_{\text{dense}}$.

IV. EXPERIMENTS

Our experiments aim to answer the following questions:

- Does our VLM-based dense reward formulation improve the efficiency of online RL? (Sec. IV-C)
- Is our autonomous RL system robust to fewer in-domain demonstrations? (Sec. IV-D)

We study tasks in both simulation and on a real robot to answer these questions, which we describe next.

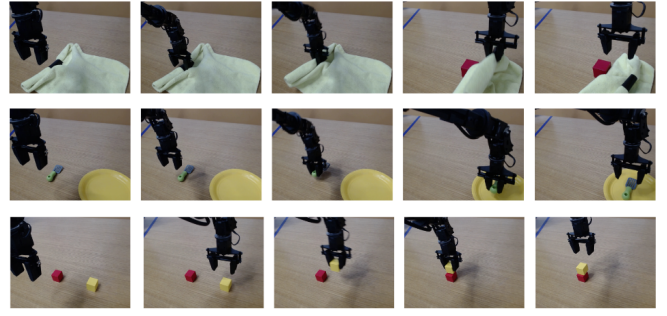


Fig. 4: **Task execution.** Evaluation is conducted in three real-world tasks: Cloth Covering, Spatula Pick-Place, and Cube Stacking.

A. Experimental Setup

Tasks. We study a simulated *Bin-Sorting* task [22], [24], where a WidowX 250 arm needs to sort objects into the correct bin specified by the language instruction. This environment is built in the PyBullet simulation framework. On a physical WidowX 250 robot arm, we study *Cloth Covering*, *Spatula Pick-Place*, and *Cube Stacking* (visualized in Fig. 4). The Cloth Covering task was introduced in RoboFuME [24], and we introduce the latter two tasks to evaluate the applicability of KAGI to new tasks. Each task consists of a forward component (e.g., uncovering the block from under the cloth) and backward component (e.g., covering the block with the cloth), and therefore can be autonomously practiced by alternating between the two sub-tasks.

Comparisons. To understand the performance without any online fine-tuning, we compare KAGI to language-conditioned behavior cloning and a pre-trained RL baseline, *CalQL* [64]. We also compare to *RoboFuME* [24], which further trains the pre-trained policy online with a sparse reward derived from a VLM success classifier. This comparison allows us to understand the benefits of the proposed dense rewards. Finally, we evaluate *MOKA* [32], which executes the trajectory defined by the VLM-generated waypoints. This last comparison does not perform any additional learning.

Datasets. All methods except for MOKA are pre-trained on a combination of trajectories selected from the Bridge dataset [62], [63] and a set of in-domain demonstrations. The in-domain demonstrations consist of 50 forward trajectories and 50 backward trajectories. Following RoboFuME [24], we additionally collect 20 failure trajectories, which are used to train the VLM-based success classifier used by RoboFuME and KAGI. In Section IV-D, we test these methods on a $5\times$ reduction in the quantity of in-domain demonstrations.

Evaluation. In both simulation and real-world evaluations, we roll out each policy for the forward task over 20 trials. For the real-world tasks, success is evaluated as follows. For Cube Covering, the entire cube must be uncovered from the camera perspective shown in Fig. 4 (left); for Spatula Pick-Place, the spatula must be on the plate; for Cube Stacking, the yellow cube must be stable atop the red cube.

B. Simulation Experiments

We conduct a preliminary test of our dense reward formulation in a simulated Bin-Sorting task, introduced in

Task	BC	Offline RL	RoboFuME	KAGI (Ours)
Cloth Covering	35%	55%	75%	75%
Spatula Pick-Place	30%	25%	40%	45%
Cube Stacking	10%	15%	25%	30%

TABLE I: Success rates over 20 trials for each method on three real-world tasks. We compare KAGI (fine-tuned for 20K steps) to offline-only methods and RoboFuME (fine-tuned for 20K steps).

RoboFuME [24]. Following their experimental setup, both RoboFuME and KAGI are provided with 10 forward and backward demonstrations, 30 failure demonstrations, and 200 total demonstrations of other pick and place tasks of diverse objects. In simulation, rewards are computed in 100×100 pixel image space. We evaluate and compare three reward formulations: dense waypoint-based only, sparse success-based only (RoboFuME), and dense + sparse (KAGI).

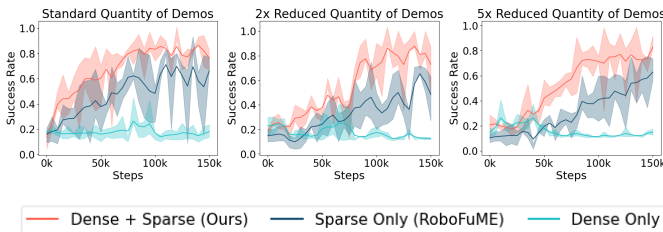


Fig. 5: Average success across 3 seeds on simulated Bin-Sorting. We evaluate each reward formulation under: the standard number of demos (left), $2\times$ reduction (middle), and $5\times$ reduction (right).

As shown in Fig. 5, **our reward formulation achieves higher success rates than the sparse-only reward formulation** that RoboFuME uses. The dense-only reward formulation performs significantly worse than the other two. This indicates that both types of rewards are necessary for efficient and successful learning: while dense rewards are useful in shaping learned behaviors, sparse rewards are also crucial to distinguish truly successful trajectories. We further test our reward formulation succeeds with a reduced number of demonstrations of the task. We test the effect of a $2\times$ reduction in demonstrations (10 forward and 10 backward demonstrations) and a $5\times$ reduction in demonstrations (4 forward and 4 backward demonstrations). In Fig. 5, we see that **our reward formulation is robust to these reductions in quantity of task demonstrations**.

C. Real-World fine-tuning with Dense Rewards

In our real-world experiments, we evaluate RoboFuME and KAGI after fine-tuning for 20K online environment training steps, with rewards computed in 640×480 pixel image space. The results are shown in Table I. For each task, RoboFuME fine-tuning improves over the offline RL policies by 10-20%, indicating further online fine-tuning is beneficial. Notably, we see lower success rates on Cube Stacking, which requires high precision and is considerably harder than the pick-place tasks in RoboFuME [24]. With KAGI, the performance further increases across the board.

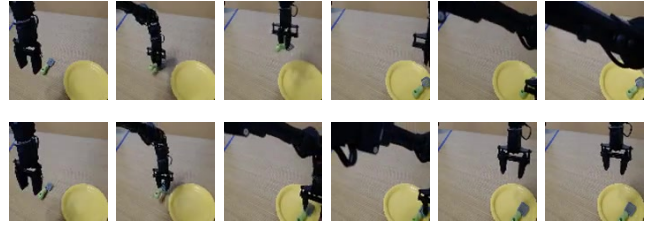


Fig. 6: Qualitative examples of policies fine-tuned with RoboFuME (top) and KAGI (bottom). RoboFuME drops the spatula from a higher height and unnecessarily moves right after. KAGI places the spatula down more gently and moves to a neutral position after.

Task	Offline RL	RoboFuME	KAGI (Ours)
Cloth Covering	45%	45%	70%
Spatula Pick-Place	10%	15%	40%
Cube Stacking	5%	15%	25%

TABLE II: Success rates over 20 trials for each method with $5\times$ fewer in-domain demonstrations. KAGI achieves similar performance to the setting with the standard amount of demonstrations, while RoboFuME performance drops with fewer demonstrations.

While the increase in success rates achieved by KAGI over RoboFuME is modest, we notice qualitatively different behaviors learned by each policy. As an example, Fig. 6 shows a representative trajectory demonstrating policy performance for Spatula Pick-Place. The policy fine-tuned with RoboFuME, while fairly successful, commonly demonstrated the behavior where the spatula was dropped onto the plate from a height, rather than lowering and placing the spatula like the demonstrations. The robot gripper also continues moving rightward rather than staying above the placement point, indicating some coincidental successes. In comparison, KAGI’s policy fine-tuned with dense shaping rewards demonstrated behavior that matched the demonstrations more closely. For more examples comparing qualitative behavior across different tasks, please see our supplementary video.

D. Robustness to Reduced In-Domain Demonstrations

Both RoboFuME and KAGI pre-train on a set of 100 in-domain demonstrations for each new task, which is a nontrivial cost. We investigate the effect of reducing the number of in-domain demonstrations used by both methods. We pre-train an offline RL policy on $5\times$ fewer than the standard quantity of in-domain demonstrations (10 forward tasks, 10 backward tasks, and 4 failures). We then fine-tune this policy online for 35K steps with RoboFuME and with KAGI. The results are shown in Table II.

Impact of reduced demos on the policy. Unsurprisingly, the offline RL policy performs worse than when trained on the standard quantity of in-domain demonstrations. Fine-tuning for 20K steps using RoboFuME marginally improves success rate over the offline RL policies, but we see a significant gap compared to its original performance with the standard number of demonstrations. For example, compared to its original success rate of 75% on Cloth Covering with 100 demos, RoboFuME only succeeds 45% of the time when given 20 demos. Therefore, the performance of

Task	MOKA with precise resets	MOKA with imprecise resets	KAGI (Ours)
Cloth Covering	90%	50%	75%
Spatula Pick-Place	70%	30%	45%
Cube Stacking	60%	15%	30%

TABLE III: Success rate of MOKA [32] with precise resets of the objects and with slight perturbations to the object positions. Without precise resets, MOKA’s performance drops significantly.

RoboFuME depends quite heavily on the amount of in-domain demonstrations provided. However, KAGI reaches its original performance even with this reduction. On the Cloth Covering task, which KAGI succeeded on 75% of the time with 100 demos, KAGI achieves a 70% success rate with 20 demos. This small drop indicates that, **even with fewer in-domain demonstrations, KAGI can recover comparable performance with more fine-tuning**. Because KAGI can tolerate fewer task-specific demonstrations, it can be applied to new tasks more easily, with a smaller data burden.

Impact of reduced demos on the success classifier.

The reduction in in-domain data also impacts the behavior of the VLM-based (MiniGPT-4) success classifier used by both RoboFuME and KAGI. We observed the sparse reward predictions of MiniGPT-4 to be significantly worse with less in-domain data to fine-tune the success predictor on. To mitigate this issue and eliminate the confounding factor of inaccurate sparse rewards, we modify RoboFuME’s [24] original sparse reward computation such that the reward predictor took four task-completion prompts as input (e.g., ‘Is the spatula on the plate?’, ‘Has the spatula been moved to the plate?’, etc.), and must reach a consensus across all prompts to generate a sparse reward of 1. This approach reduces the number of false positives, which RL algorithms often exploit. This reveals another source of fragility in the system, as fine-tuning MiniGPT-4 is heavily reliant on in-domain demonstrations to generate accurate sparse rewards crucial for online RL. Leveraging larger models like GPT-4V that have stronger zero-shot performance to extract sparse task completion rewards may help circumvent this issue.

E. Importance of Online Fine-tuning

Since the VLM prompting component of KAGI is inspired by MOKA [32], we additionally evaluate MOKA to understand whether online fine-tuning offers any advantages. MOKA [32] leverages GPT-4V to predict affordance keypoints and plan a sequence of action primitives (e.g., ‘lift’, ‘reach grasp’, ‘grasp’), then directly executes the action primitive sequence by computing the actions required to reach each point. We evaluate two versions of MOKA: the first with precise resets that closely match the inputs to the VLM, and the second with slight perturbations to these initial conditions that is representative of environment resets after backward policy rollouts. The purpose of this comparison is to understand whether the VLM-generated keypoints can be reused for different initial conditions in both methods, since the cost of querying GPT-4V for every new condition

is prohibitively high. Compared to this, KAGI only queries for keypoints and waypoint trajectories once at the start of online training. In Table III, we see that MOKA with precise resets succeeds between 60% to 90% of the time depending on the task, which actually is better than the performance of our policy. However, without these precise resets, the performance of MOKA drops noticeably, which means the GPT-4V keypoints are not reusable for this method when there are even slight perturbations to the environment, since actions are computed directly with respect to these keypoints. However, KAGI can recover some of this performance loss with online fine-tuning, without the cost of additional GPT-4V queries. KAGI leverages the benefits of closed-loop systems that are more generalizable and robust to environment changes, as opposed to open-loop systems that use hand-designed action primitives. This makes, KAGI more suitable for the autonomous RL paradigm, which involves potentially imperfect policy rollouts on a real robot.

V. CONCLUSION & FUTURE WORK

Our experiments present several insights into the opportunities and challenges of autonomous RL pipelines, and the potential of mark-based visual prompting for improving generalization capabilities of robots equipped with RL. In particular, we explore the challenges of using only sparse rewards for online fine-tuning and relying on in-domain demonstrations with low multimodality to pre-train policies for online RL. Approaches using only sparse rewards are slower to learn to complete tasks, and approaches reliant on in-domain demonstrations are much more brittle and less robust to generalizing to new tasks, objects, and environments.

We demonstrate that dense shaping rewards extracted from VLMs can help speed up online RL, and facilitate generalization to new tasks where relying only on sparse rewards is less efficient. Leveraging both dense and sparse rewards improves autonomous learning, with better robustness to reduced in-domain demonstrations than sparse rewards alone. Our reward formulation is a possible modification to make existing fine-tuning methods more robust and data-efficient. Our work has demonstrated the benefits of VLM-based dense shaping rewards, and opens up new avenues of exploration to harness the generalization capabilities of VLMs to enhance the robustness of robot learning systems.

There are several areas for future work. First, sparse task completion rewards only track if the object reached the target location or not; incorporating waypoint trajectories for object tracking into the dense reward computation could further expedite learning. In addition, running large models like GPT-4V after every episode to generate rewards might be more accurate, but is extremely costly and suffers from latency issues, and future work can explore this tradeoff. Finally, further hyperparameter tuning in the dense reward computation and CalQL algorithm could improve the success rate of policies fine-tuned with dense and sparse rewards. Overall, these research directions can help efficiently scale autonomous RL systems to a greater diversity of complex tasks with different objects and environments.

REFERENCES

- [1] OpenAI, “Gpt-4 technical report,” in *arXiv preprint arXiv:2303.08774*, 2023.
- [2] A. Chowdhery, S. Narang, J. Devlin, M. Bosma, G. Mishra, A. Roberts, P. Barham, H. W. Chung, C. Sutton, S. Gehrmann, P. Schuh, K. Shi, S. Tsvyashchenko, J. Maynez, A. Rao, P. Barnes, Y. Tay, N. Shazeer, V. Prabhakaran, E. Reif, N. Du, B. Hutchinson, R. Pope, J. Bradbury, J. Austin, M. Isard, G. Gur-Ari, P. Yin, T. Duke, A. Levskaya, S. Ghemawat, S. Dev, H. Michalewski, X. Garcia, V. Misra, K. Robinson, L. Fedus, D. Zhou, D. Ippolito, D. Luan, H. Lim, B. Zoph, A. Spiridonov, R. Sepassi, D. Dohan, S. Agrawal, M. Omernick, A. M. Dai, T. S. Pillai, M. Pellat, A. Lewkowycz, E. Moreira, R. Child, O. Polozov, K. Lee, Z. Zhou, X. Wang, B. Saeta, M. Diaz, O. Firat, M. Catasta, J. Wei, K. Meier-Hellstern, D. Eck, J. Dean, S. Petrov, and N. Fiedel, “Palm: scaling language modeling with pathways,” *Journal of Machine Learning Research*, vol. 24, no. 1, 2024.
- [3] M. Ahn, A. Brohan, N. Brown, Y. Chebotar, O. Cortes, B. David, C. Finn, C. Fu, K. Gopalakrishnan, K. Hausman *et al.*, “Do as i can, not as i say: Grounding language in robotic affordances,” in *Conference on Robot Learning*, 2022.
- [4] A. Radford, J. W. Kim, C. Hallacy, A. Ramesh, G. Goh, S. Agarwal, G. Sastry, A. Askell, P. Mishkin, J. Clark, G. Krueger, and I. Sutskever, “Learning transferable visual models from natural language supervision,” in *arXiv preprint arXiv:2103.00020*, 2021.
- [5] J. Li, D. Li, C. Xiong, and S. C. H. Hoi, “Blip: Bootstrapping language-image pre-training for unified vision-language understanding and generation,” in *International Conference on Machine Learning*, 2022.
- [6] D. Driess, F. Xia, M. S. M. Sajjadi, C. Lynch, A. Chowdhery, B. Ichter, A. Wahid, J. Tompson, Q. Vuong, T. Yu, W. Huang, Y. Chebotar, P. Sermanet, D. Duckworth, S. Levine, V. Vanhoucke, K. Hausman, M. Toussaint, K. Greff, A. Zeng, I. Mordatch, and P. Florence, “Palm-e: An embodied multimodal language model,” in *arXiv preprint arXiv:2303.03378*, 2023.
- [7] A. Brohan, N. Brown, J. Carbajal, Y. Chebotar, X. Chen, K. Choremanski, T. Ding, D. Driess, A. Dubey, C. Finn *et al.*, “Rt-2: Vision-language-action models transfer web knowledge to robotic control,” *arXiv preprint arXiv:2307.15818*, 2023.
- [8] B. Chen, F. Xia, B. Ichter, K. Rao, K. Gopalakrishnan, M. S. Ryoo, A. Stone, and D. Kappler, “Open-vocabulary queryable scene representations for real world planning,” in *IEEE International Conference on Robotics and Automation*. IEEE, 2023, pp. 11 509–11 522.
- [9] W. Huang, P. Abbeel, D. Pathak, and I. Mordatch, “Language models as zero-shot planners: Extracting actionable knowledge for embodied agents,” *arXiv preprint arXiv:2201.07207*, 2022.
- [10] W. Huang, F. Xia, T. Xiao, H. Chan, J. Liang, P. Florence, A. Zeng, J. Tompson, I. Mordatch, Y. Chebotar, P. Sermanet, N. Brown, T. Jackson, L. Luu, S. Levine, K. Hausman, and B. Ichter, “Inner monologue: Embodied reasoning through planning with language models,” in *Conference on Robot Learning*, 2022.
- [11] J. Yang, H. Zhang, F. Li, X. Zou, C. Li, and J. Gao, “Set-of-mark prompting unleashes extraordinary visual grounding in gpt-4v,” *arXiv preprint arXiv:2310.11441*, 2023.
- [12] B. Chen, Z. Xu, S. Kirmani, B. Ichter, D. Driess, P. Florence, D. Sadigh, L. Guibas, and F. Xia, “Spatialvlm: Endowing vision-language models with spatial reasoning capabilities,” in *Conference on Computer Vision and Pattern Recognition*, 2024.
- [13] S. Nasiriany, F. Xia, W. Yu, T. Xiao, J. Liang, I. Dasgupta, A. Xie, D. Driess, A. Wahid, Z. Xu *et al.*, “Pivot: Iterative visual prompting elicits actionable knowledge for vlms,” *arXiv preprint arXiv:2402.07872*, 2024.
- [14] S. Mirchandani, F. Xia, P. Florence, B. Ichter, D. Driess, M. G. Arenas, K. Rao, D. Sadigh, and A. Zeng, “Large language models as general pattern machines,” in *Conference on Robot Learning*, 2023.
- [15] Y.-J. Wang, B. Zhang, J. Chen, and K. Sreenath, “Prompt a robot to walk with large language models,” *arXiv preprint arXiv:2309.09969*, 2023.
- [16] Y. Jiang, A. Gupta, Z. Zhang, G. Wang, Y. Dou, Y. Chen, L. Fei-Fei, A. Anandkumar, Y. Zhu, and L. Fan, “Vima: General robot manipulation with multimodal prompts,” in *Fortieth International Conference on Machine Learning*, 2023.
- [17] R. Li, L. B. Allal, Y. Zi, N. Muennighoff, D. Kocetkov, C. Mou, M. Marone, C. Akiki, J. Li, J. Chim, Q. Liu, E. Zheltonozhskii, T. Y. Zhuo, T. Wang, O. Dehaene, M. Davoodi, J. Lamy-Poirier, J. Monteiro, O. Shliazhko, N. Gontier, N. Meade, A. Zebaze, M.-H. Yee, L. K. Umapathi, J. Zhu, B. Lipkin, M. Oblokulov, Z. Wang, R. Murthy, J. Stillerman, S. S. Patel, D. Abulkhanov, M. Zocca, M. Dey, Z. Zhang, N. Fahmy, U. Bhattacharyya, W. Yu, S. Singh, S. Luccioni, P. Villegas, M. Kunakov, F. Zhdanov, M. Romero, T. Lee, N. Timor, J. Ding, C. Schlesinger, H. Schoelkopf, J. Ebert, T. Dao, M. Mishra, A. Gu, J. Robinson, C. J. Anderson, B. Dolan-Gavitt, D. Contractor, S. Reddy, D. Fried, D. Bahdanau, Y. Jernite, C. M. Ferrandis, S. Hughes, T. Wolf, A. Guha, L. von Werra, and H. de Vries, “Starcode: may the source be with you!” in *Transactions on Machine Learning Research (TMLR)*, 2023.
- [18] J. Liang, W. Huang, F. Xia, P. Xu, K. Hausman, B. Ichter, P. Florence, and A. Zeng, “Code as policies: Language model programs for embodied control,” in *arXiv preprint arXiv:2209.07753*, 2022.
- [19] A. Kumar, A. Zhou, G. Tucker, and S. Levine, “Conservative q-learning for offline reinforcement learning,” *Advances in Neural Information Processing Systems*, vol. 33, pp. 1179–1191, 2020.
- [20] A. Nair, A. Gupta, M. Dalal, and S. Levine, “Awac: Accelerating online reinforcement learning with offline datasets,” in *arXiv preprint arXiv:2006.09359*, 2021.
- [21] I. Kostrikov, A. Nair, and S. Levine, “Offline reinforcement learning with implicit q-learning,” *arXiv preprint arXiv:2110.06169*, 2021.
- [22] A. Kumar, A. Singh, F. Ebert, M. Nakamoto, Y. Yang, C. Finn, and S. Levine, “Pre-training for robots: Offline rl enables learning new tasks in a handful of trials,” in *Robotics: Science and Systems*, 2022.
- [23] M. S. Mark, A. Ghadrizadeh, X. Chen, and C. Finn, “Fine-tuning of offline policies with optimistic action selection,” in *Deep Reinforcement Learning Workshop NeurIPS 2022*, 2022.
- [24] J. Yang, M. S. Mark, B. Vu, A. Sharma, J. Bohg, and C. Finn, “Robot fine-tuning made easy: Pre-training rewards and policies for autonomous real-world reinforcement learning,” in *2024 IEEE International Conference on Robotics and Automation*. IEEE, 2024.
- [25] J. Ho and S. Ermon, “Generative adversarial imitation learning,” *Advances in Neural Information Processing Systems*, vol. 29, 2016.
- [26] J. Fu, K. Luo, and S. Levine, “Learning robust rewards with adversarial inverse reinforcement learning,” in *International Conference on Learning Representations*, 2018.
- [27] J. Fu, A. Singh, D. Ghosh, L. Yang, and S. Levine, “Variational inverse control with events: A general framework for data-driven reward definition,” *Advances in Neural Information Processing Systems*, vol. 31, 2018.
- [28] A. Xie, A. Singh, S. Levine, and C. Finn, “Few-shot goal inference for visuomotor learning and planning,” in *Conference on Robot Learning*, 2018, pp. 40–52.
- [29] A. Singh, L. Yang, K. Hartikainen, C. Finn, and S. Levine, “End-to-end robotic reinforcement learning without reward engineering,” in *Robotics: Science and Systems*, 2019.
- [30] P. Mahmoudieh, D. Pathak, and T. Darrell, “Zero-shot reward specification via grounded natural language,” in *Proceedings of the 39th International Conference on Machine Learning*, vol. 162. PMLR, 2022, pp. 14 743–14 752.
- [31] A. Villa, J. L. Alcázar, M. Alfarra, K. Alhamoud, J. Hurtado, F. C. Heilbron, A. Soto, and B. Ghanem, “Pivot: Prompting for video continual learning,” in *2023 IEEE/CVF Conference on Computer Vision and Pattern Recognition*, 2023, pp. 24 214–24 223.
- [32] K. Fang, F. Liu, P. Abbeel, and S. Levine, “Moka: Open-world robotic manipulation through mark-based visual prompting,” in *Robotics: Science and Systems*, 2024.
- [33] R. B. *et al.*, “On the opportunities and risks of foundation models,” in *arXiv preprint arXiv:2108.07258*, 2022.
- [34] A. Zeng, M. Attarian, B. Ichter, K. Choremanski, A. Wong, S. Welker, F. Tombari, A. Purohit, M. Ryoo, V. Sindhwani, J. Lee, V. Vanhoucke, and P. Florence, “Socratic models: Composing zero-shot multimodal reasoning with language,” in *International Conference on Learning Representations*, 2023.
- [35] S. S. Raman, V. Cohen, E. Rosen, I. Idrees, D. Paulius, and S. Tellex, “Planning with large language models via corrective re-prompting,” in *Foundation Models for Decision Making Workshop at NeurIPS 2022*, 2022.
- [36] T. Silver, S. Dan, K. Srinivas, J. B. Tenenbaum, L. P. Kaelbling, and M. Katz, “Generalized planning in pddl domains with pretrained large language models,” in *AAAI Conference on Artificial Intelligence*, 2023.
- [37] K. Lin, C. Agia, T. Migimatsu, M. Pavone, and J. Bohg, “Text2motion: from natural language instructions to feasible plans,” *Autonomous Robots*, Nov 2023.

- [38] V. S. Dorbala, G. Sigurdsson, R. Piramuthu, J. Thomason, and G. S. Sukhatme, "Clip-nav: Using clip for zero-shot vision-and-language navigation," in *arXiv preprint arXiv:2211.16649*, 2022.
- [39] D. Shah, B. Osinski, B. Ichter, and S. Levine, "LM-nav: Robotic navigation with large pre-trained models of language, vision, and action," in *6th Annual Conference on Robot Learning*, 2022.
- [40] C. Huang, O. Mees, A. Zeng, and W. Burgard, "Visual language maps for robot navigation," in *Proceedings of the IEEE International Conference on Robotics and Automation*, London, UK, 2023.
- [41] A. Brohan, N. Brown, J. Carbajal, Y. Chebotar, X. Chen, K. Choremanski, T. Ding, D. Driess, A. Dubey, C. Finn, P. Florence, C. Fu, M. G. Arenas, K. Gopalakrishnan, K. Han, K. Hausman, A. Herzog, J. Hsu, B. Ichter, A. Irpan, N. Joshi, R. Julian, D. Kalashnikov, Y. Kuang, I. Leal, L. Lee, T.-W. E. Lee, S. Levine, Y. Lu, H. Michalewski, I. Mordatch, K. Pertsch, K. Rao, K. Reymann, M. Ryoo, G. Salazar, P. Sanketi, P. Sermanet, J. Singh, A. Singh, R. Soricut, H. Tran, V. Vanhoucke, Q. Vuong, A. Wahid, S. Welker, P. Wohlhart, J. Wu, F. Xia, T. Xiao, P. Xu, S. Xu, T. Yu, and B. Zitkovich, "Rt-2: Vision-language-action models transfer web knowledge to robotic control," in *arXiv preprint arXiv:2307.15818*, 2023.
- [42] J. Gu, S. Kirmani, P. Wohlhart, Y. Lu, M. G. Arenas, K. Rao, W. Yu, C. Fu, K. Gopalakrishnan, Z. Xu, P. Sundaresan, P. Xu, H. Su, K. Hausman, C. Finn, Q. Vuong, and T. Xiao, "Rt-trajectory: Robotic task generalization via hindsight trajectory sketches," 2023.
- [43] Y. Hong, H. Zhen, P. Chen, S. Zheng, Y. Du, Z. Chen, and C. Gan, "3d-llm: Injecting the 3d world into large language models," in *Advances in Neural Information Processing Systems*, 2023.
- [44] H. Huang, Z. Wang, R. Huang, L. Liu, X. Cheng, Y. Zhao, T. Jin, and Z. Zhao, "Chat-3d v2: Bridging 3d scene and large language models with object identifiers," *arXiv preprint arXiv:2312.08168*, 2023.
- [45] Z. Wang, H. Huang, Y. Zhao, Z. Zhang, and Z. Zhao, "Chat-3d: Data-efficiently tuning large language model for universal dialogue of 3d scenes," *arXiv preprint arXiv:2308.08769*, 2023.
- [46] W. Huang, C. Wang, R. Zhang, Y. Li, J. Wu, and L. Fei-Fei, "Voxposer: Composable 3d value maps for robotic manipulation with language models," *arXiv preprint arXiv:2307.05973*, 2023.
- [47] J. Yang, X. Chen, N. Madaan, M. Iyengar, S. Qian, D. F. Fouhey, and J. Chai, "3d-grand: A million-scale dataset for 3d-llms with better grounding and less hallucination," in *arXiv preprint arXiv:2406.05132*, 2024.
- [48] Z. Yang, L. Li, K. Lin, J. Wang, C.-C. Lin, Z. Liu, and L. Wang, "The dawn of llms: Preliminary explorations with gpt-4v(ision)," in *arXiv preprint arXiv:2309.17421*, 2023.
- [49] G. T. Google, "Gemini: A family of highly capable multimodal models," in *arXiv preprint arXiv:2312.11805*, 2024.
- [50] W. Huang, C. Wang, Y. Li, R. Zhang, and L. Fei-Fei, "Rekep: Spatio-temporal reasoning of relational keypoint constraints for robotic manipulation," in *Conference on Robot Learning*, 2024.
- [51] M. Minderer, A. Gritsenko, A. Stone, M. Neumann, D. Weissenborn, A. Dosovitskiy, A. Mahendran, A. Arnab, M. Dehghani, Z. Shen, X. Wang, X. Zhai, T. Kipf, and N. Houlsby, "Simple open-vocabulary object detection with vision transformers," in *arXiv preprint arXiv:2205.06230*, 2022.
- [52] T. Ren, S. Liu, A. Zeng, J. Lin, K. Li, H. Cao, J. Chen, X. Huang, Y. Chen, F. Yan, Z. Zeng, H. Zhang, F. Li, J. Yang, H. Li, Q. Jiang, and L. Zhang, "Grounded sam: Assembling open-world models for diverse visual tasks," in *arXiv preprint arXiv:2401.14159*, 2024.
- [53] A. Sharma, K. Xu, N. Sardana, A. Gupta, K. Hausman, S. Levine, and C. Finn, "Autonomous reinforcement learning: Formalism and benchmarking," in *International Conference on Learning Representations*, 2022.
- [54] M. Balsells, M. Torne, Z. Wang, S. Desai, P. Agrawal, and A. Gupta, "Autonomous robotic reinforcement learning with asynchronous human feedback," in *Conference on Robot Learning*, 2023.
- [55] A. Gupta, J. Yu, T. Z. Zhao, V. Kumar, A. Rovinsky, K. Xu, T. Devlin, and S. Levine, "Reset-free reinforcement learning via multi-task learning: Learning dexterous manipulation behaviors without human intervention," in *2021 IEEE International Conference on Robotics and Automation*, 2021, pp. 6664–6671.
- [56] C. Sun, J. Orvik, C. M. Devin, B. H. Yang, A. Gupta, G. Berseth, and S. Levine, "Fully autonomous real-world reinforcement learning with applications to mobile manipulation," in *Proceedings of the 5th Conference on Robot Learning*, ser. Proceedings of Machine Learning Research, vol. 164. PMLR, 2022, pp. 308–319.
- [57] D. Zhu, J. Chen, X. Shen, X. Li, and M. Elhoseiny, "Minigpt-4: Enhancing vision-language understanding with advanced large language models," in *International Conference on Learning Representations*, 2024.
- [58] Y. J. Ma, W. Liang, G. Wang, D.-A. Huang, O. Bastani, D. Jayaraman, Y. Zhu, L. Fan, and A. Anandkumar, "Eureka: Human-level reward design via coding large language models," in *International Conference on Learning Representations*, 2024.
- [59] W. Yu, N. Gileadi, C. Fu, S. Kirmani, K.-H. Lee, M. G. Arenas, H.-T. L. Chiang, T. Erez, L. Hasenclever, J. Humplik, B. Ichter, T. Xiao, P. Xu, A. Zeng, T. Zhang, N. Heess, D. Sadigh, J. Tan, Y. Tassa, and F. Xia, "Language to rewards for robotic skill synthesis," in *Conference on Robot Learning*, 2023.
- [60] H. Xiong, R. Mendonca, K. Shaw, and D. Pathak, "Adaptive mobile manipulation for articulated objects in the open world," *arXiv preprint arXiv:2401.14403*, 2024.
- [61] N. Karaev, I. Rocco, B. Graham, N. Neverova, A. Vedaldi, and C. Rupprecht, "Cotracker: It is better to track together," in *European Conference on Computer Vision*, 2024.
- [62] F. Ebert, Y. Yang, K. Schmeckpeper, B. Bucher, G. Georgakis, K. Daniilidis, C. Finn, and S. Levine, "Bridge data: Boosting generalization of robotic skills with cross-domain datasets," in *Robotics: Science and Systems*, 2022.
- [63] H. Walke, K. Black, A. Lee, M. J. Kim, M. Du, C. Zheng, T. Zhao, P. Hansen-Estruch, Q. Vuong, A. He, V. Myers, K. Fang, C. Finn, and S. Levine, "Bridgedata v2: A dataset for robot learning at scale," in *Conference on Robot Learning*, 2023.
- [64] M. Nakamoto, Y. Zhai, A. Singh, M. S. Mark, Y. Ma, C. Finn, A. Kumar, and S. Levine, "Cal-ql: Calibrated offline rl pre-training for efficient online fine-tuning," in *Advances in Neural Information Processing Systems*, 2023.